# Chapter 10
# Ionospheric Anomalies During the March 2013 Geomagnetic Storm from BeiDou Navigation Satellite System (BDS) Observations

**Rui Jin, Shuanggen Jin and Xuelin Tao**

**Abstract** Earth's ionosphere disturbances triggered by the geomagnetic storm usually affect the propagation of radio electromagnetic wave. The mid-geomagnetic storm occurred in March 2013 with Dst index of up to $-132$ nT, which may disturb signal tracking and positioning results of Global Navigation Satellite Systems (GNSS). Unfortunately, LOS TEC series derived from GPS observations contain the ionospheric horizontal gradient information due to the satellites' movement. Geosynchronous Earth orbit (GEO) satellites of BeiDou navigation satellite system (BDS) give us an opportunity to detect ionospheric variations without horizontal gradient of electron density affection. In this paper, the Beidou stations' data provided by multi-GNSS experiments (MGEX) from IGS are the first time used to analyze the geomagnetic storm effects on Beidou navigation system (BDS) and ionospheric anomalous behaviors during 15–21 March 2013. The total electron content (TEC) variations are investigated during this geomagnetic storm using carrier phase measurements from BeiDou GEO satellites in B1 and B2. Dramatic TEC decrease is observed at the main storm and then increases gradually. Hourly TEC scintillation enhances greatly in the next hours of Storm Sudden Commencements (SSC). Although geomagnetic storm effect is global and regional, anomalies difference also can be detected by BDS-GEO TEC observations.

**Keywords** BDS · Total electron content · Geomagnetic storm · Ionospheric behaviors

R. Jin (✉)
Shanghai Astronomical Observatory, Chinese Academy of Sciences, Shanghai, China
e-mail: ruijin@shao.ac.cn

R. Jin · S. Jin
Graduate University of Chinese Academy of Sciences, Beijing, China
e-mail: sgjin@shao.ac.cn

X. Tao
School of Civil Engineering, Hefei University of Technology, Hefei, China

## 10.1 Introduction

As we know, Earth's ionosphere is dispersive medium. Phases and amplitudes of electro-magnetic wave will be disturbed during its propagation in the ionosphere. Basing on the refraction principles, the dual-frequencies observation of Global Navigation Satellite Systems (GNSS) can be used to monitor the Earth's ionosphere [1–3]. After the recent decades development, GNSS ionosphere monitoring has been become one of the most important GNSS applications. Comparing to traditional ionosphere detection, GNSS ionosphere monitoring has better temporal-spatial resolution. Up to now, GNSS ionosphere monitoring has two approaches through GNSS observations. One is the Earth's ionosphere total electron content (TEC) modelling from ground-based GNSS observations, another way is used by the space-borne GNSS radio occultation. Since 1998, International GNSS Services (IGS) has been continually providing Global TEC maps derived from global consciously operating GNSS stations' data [4, 5]. Regional TEC models with high temporal-spatial resolution has also been built up using GNSS dual-frequencies data with the advent of dense GNSS network, such as continuous GPS network in Japan (GEONET) [6]. The ground-based GNSS derived TEC models not only play an important role in error correction of GNSS positioning, navigation and timing (PNT), especially for single-frequencies users, but also are a reliable source for the study of large and middle scale ionospheric variations. What's more GNSS ionospheric TEC has been the important input of international reference ionosphere model (IRI) [7, 8]. The GNSS ionosphere study mainly focuses on anomaly analysis of TEC along the GNSS signal travelling light of sight (LOS), such as ionospheric effects of solar activities, geomagnetic storms, earthquakes, tsunami, ballistic missiles and some other natural and artificial events [9–13]. Most of GNSS TEC models used for ionospheric delay correction can work well during quiet days, while its precision will be decreased on disturbed days due to the ionospheric effects caused by the events mentioned above. Therefore, on one hand, GNSS ionospheric monitoring can improve ionospheric delay correction of electro-magnetic wave propagation. On the other hand, it has great potentials in disaster warning and space weather motoring.

Usually, the LOS TEC from GPS is used for small scale ionospheric anomaly and rapid change analysis. Unfortunately, LOS TEC series derived from GNSS observations contains the ionospheric horizontal gradient information due to the satellites' movement. It is difficult to divide the TEC variations at one pierce point accurately in Earth Centered Earth Fixed coordinate system (ECEF). Geosynchronous orbit (GEO) satellites of BDS give us an opportunity to detect ionospheric variations without horizontal gradient of electron density affection. In this paper, we analyze the rapid ionospheric behaviours and responses to the geomagnetic storm happened in March 2013 using BDS data from multi-GNSS experiment (MGEX). In Sect. 10.2, the sub-storm in March 2013 is introduced and BDS-GEO TEC estimates are given. Section 10.3 shows the ionospheric effects detected by BDS GEO observations during this geomagnetic storm. And Sect. 10.4 is the summary and conclusions.

## 10.2  Geomagnetic Storm in March 2013 and BDS-GEO TEC Monitoring

A moderate geomagnetic storm occurred in the middle of March in 2013. Figure 10.1 shows the Dst, AE and Ap index variation in March 2013. Dst and AE data is provided by World Data Center (WDC) for Geomagnetism, Kyoto (http://wdc.kugi.kyoto-u.ac.jp/). Dst index released by WDC is derived by the observations of geomagnetic field horizontal component H getting from magnetic observatories, Hermanus, Kakioka, Honolulu, and San Juan, which are located around the 20°S and 20°N where are sufficiently far from the auroral and equatorial electrojets. Dst index is a good indicator for the disturbance of mid-latitude and near-equatorial geomagnetic field. AE index is extracted from the magnetic field horizontal component observed by 10–13 magnetic observatories located in auroral zone in the northern hemisphere, which reflects the magnetic field variation in the auroral region as the result of electric currents flowing in the high-latitude ionosphere. Ap index presented in Fig. 10.1 is provided by GeoForschungsZentrum (GFZ) (http://www.gfz-potsdam.de/). Ap index is a linear scale from Kp index, which is derived from magnetic field horizontal field components observed by 13 subauroral magnetic stations. As shown in Fig. 10.1, the main disturbances of Dst, AE and Ap index appear on March 17. The Earth's magnetic field is disturbed dramatically in the near-equatorial, mid-latitude and auroral regions. The peak value of Dst index is up to −136 nT. This event is a moderate geomagnetic storm according to NOAA space weather scales.

Here we intend to use BDS-GEO TEC to analyze the ionospheric effects. Three MGEX BDS tracking stations are used (Table 10.1). All of these BDS stations have a good view for BDS GEO satellites.

The TEC along the signal propagation path can be derived from BDS dual-frequencies observations using Eq. (10.1). Here high-orders of refraction index and path differences in two bands are ignored [14].

$$TEC = \frac{f_1^2 f_2^2}{40.28 \left(f_1^2 - f_2^2\right)} (L_1 - L_2 + const_L) = \frac{f_1^2 f_2^2}{40.28 \left(f_2^2 - f_1^2\right)} (P_1 - P_2 - const_P)$$

(10.1)

where $f$ stands for signal frequency, $L$ and $P$ stand for BDS carries phase and pseudorange measurements, $const_L$ and $const_P$ are constant items for one continuous observation arc, such as clock error, instrument biases, ambiguity (only for $const_L$) and multipath effects. Based on the thin shell ionosphere assumption, TEC can be converted to vertical TEC using the simple cosine mapping function as follow [15]:

$$vTEC = TEC * \cos\left(\arcsin\left(\frac{R \sin z}{R + H}\right)\right)$$

(10.2)

**Fig. 10.1** Dst, AE and Ap index variations during March in 2013. The Dst and AE index data are provided by WDC center, while Ap index is provided by GFZ
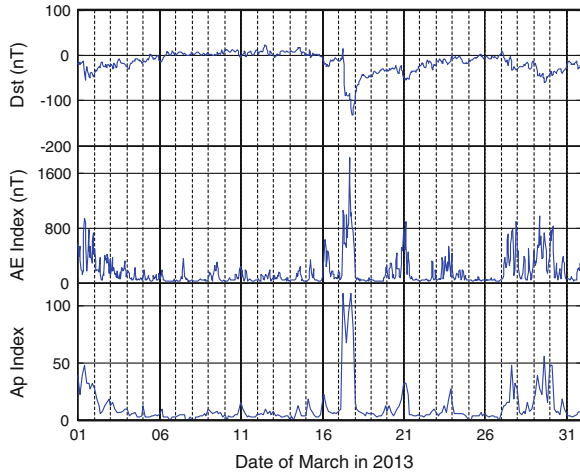


**Table 10.1** Basic information of the 3 chosen MGEX BDS stations

| Station name | Latitude/° | Longitude/° | Height/m | Receiver | Country |
|---|---|---|---|---|---|
| cut0 | −32.00 | 115.50 | 24.0 | Trimble NetR9 | Australia |
| gmsd | 30.56 | 131.02 | 142.6 | Trimble NetR9 | Japan |
| jfng | 30.52 | 114.49 | 71.3 | Trimble NetR9 | China |

where $R$ is the radius of Earth, $z$ is zenith distance of signal path at the ionospheric pierce point, and $H$ is the thin shell ionosphere height. Usually the height is set as 300–500 km that is the maximum electron density height of F2 layer. Here the height of 350 km is used. We use carrier phase observations to get TEC values because of its higher precision when compared to pseudorange observations. The relative location between BDS stations and BDS GEO satellites almost do not change. GEO satellites will be available permanently for BDS stations when the satellites and tracking stations are operating normally. For one continuous arc, the constant item in Eq. (10.1) will not change (ignore the measurement error of carrier phase observations). It can be removed by adding the difference between the TEC series derived from global ionosphere map (GIM). The ionospheric effects of moderate geomagnetic storm occurred in March 2013 will be analyzed using BDS-GEO TEC in next section.

## 10.3  Results and Discussion

Figure 10.2 shows the TEC time series derived from C01 (GEO-1) satellite's dual frequencies carrier phase observations on band B1 and B2 at MGEX cut0 station during the geomagnetic storm in March 2013. The location of cut0 station is shown in Table 10.1. BDS C01 is on the Earth-synchronous orbit with 140°E. The IPP is located at 29.7°S, 118.1°E. In quiet days, for one fixed point in ECEF, TEC values vary at about a constant with small floating amplitude at the same epoch of adjacent days. In general, one point TEC variation at same epoch of days is floating quasi-random around a constant in short period. So it is reasonable to use 2 times of standard deviation of previous 5 days corresponding TEC value as the anomaly threshold. When the TEC values are out of the 2 times standard deviation range, we thought the ionospheric anomaly occurs. As shown in Fig. 10.2 (left), the blue line is the upper boundary that is the sum of mean value and 2 times standard deviation of the same epoch observations of 5 days before the current day. And the red line is the lower boundary that is the difference of mean value and 2 times standard deviation. The boundary lines are incomplete during March 15–17, which is caused by lacking observation on corresponding epochs. The green line stands for the TEC variation from March 15 to March 21. The black dash line is the Storm Sudden Commencements (SSC) released by International Association of Geomagnetism and Aeronomy (IAGA). Dramatic TEC decrease can be found after the SSC and then increase gradually. This trend contains the effect of solar radio flux variation caused by Carrington rotation whose period is nearly 27 days. However it will not cause a sudden decease in normal condition. It is clear to see that the TEC value is out of the 2 times standard deviation from the SSC to the early of March 18. The difference of TEC values and its upper and lower threshold and the radio between the difference and mean values of pervious 5 days are shown on the right panel of Fig. 10.2. The negative anomalies can even be up to about 20 TECU, which is approximately 60 % of the mean value of previous days.

Figures 10.3 and 10.4 for stations gmsd and jfng are similar with Fig. 10.2. These two stations are almost located on the same latitude line. Their anomaly amplitude is similar with about 5 TECU (10–20 %). The anomalies mainly occur on 1–2 days after the SSC. Comparing to quasi conjunction IPP observed by cut0–C01, the anomaly amplitude is much smaller. In general, the ionospheric effects of geomagnetic storm in March 2013 is negative anomalies occurring on 1–2 days after the SSC, while the anomalies amplitudes is difference at different locations.

Figure 10.5 is the hourly standard deviation of the detrended TEC rate (TECU/min) at these three IPPs from March 15 to March 21. Comparing to the same time of pervious and next days, hourly TEC scintillation enhancement in the several hours after SSC can be seen, especially for IPP (29.8°S, 118.1°E) observed by cut0–C01. For IPP (29.8°S, 118.1°E), the enhancement starts from UT 8–20. For the other two IPPs, the enhancement is mainly occurring at UT 10–13.
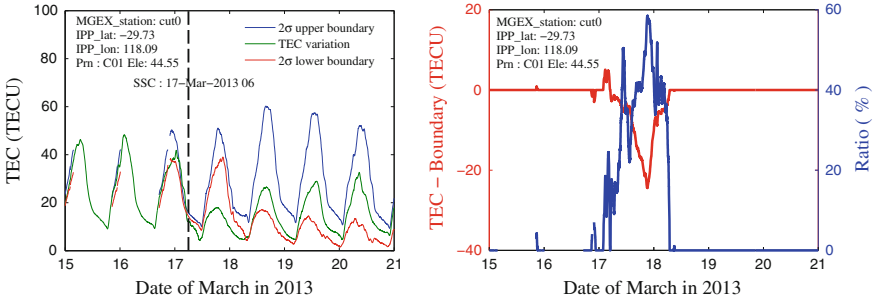
**Fig. 10.2** TEC variation at MGEX station cut0 during the geomagnetic storm in March 2013. The *upper* and *lower* boundary is derived from the same epoch of 5 days observations before the event. The *black dash line* stands for storm sudden commencements provided by international service of geomagnetic indices
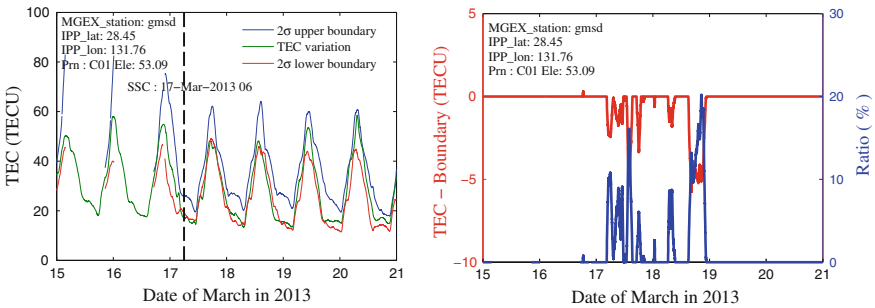


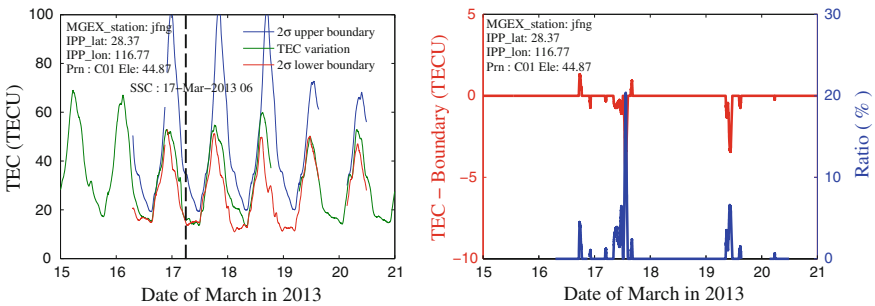**Fig. 10.3** MGEX station gmsd TEC anomalies during the geomagnetic storm in March 2013



**Fig. 10.4** MGEX station jfng absolute TEC variation during the geomagnetic storm in March 2013
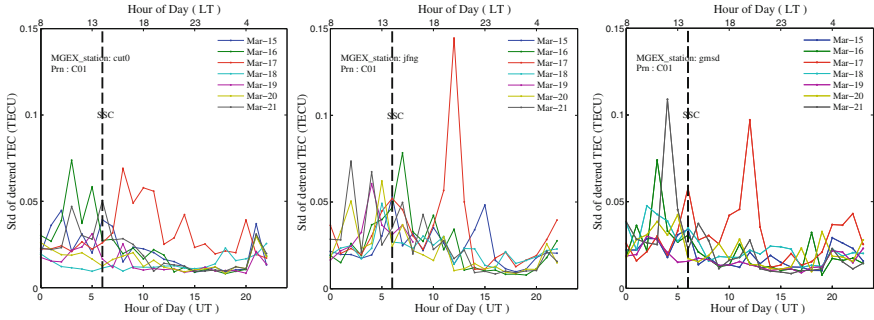
**Fig. 10.5** Hourly standard deviation of the detrended TEC rate at MGEX statiosn cut0 (*left*), jfng (*middle*) and gmsd (*right*) with C01 (GEO-1). The *bottom* x-axis stands for the Universal Time (*UT*) while the *top* x-axis stands for local time corresponding to the IPP location

As shown in Fig. 10.5, during UT 1–6, the hourly standard deviation is higher than other periods and its difference between adjacent days is also much larger, which may be related to the local time variation.

## 10.4  Summary and Conclusions

This paper is the first time to use BDS-GEO observations to analyze the ionospheric effect of a moderate geomagnetic storm. Since the location of GEO satellites and the BDS tracking station in ECEF almost do not change, it provides us a unique opportunity to measure continuous TEC variations at one point without TEC horizontal gradient caused by IPP's variation. Three MGEX BDS stations cut0, gmsd and jfng are used to study the TEC variation in Asia/Pacific region during the storm. The results show that TEC values decrease dramatically after the SSC and increase gradually during the recovery phase of the storm. Obvious anomalies mainly occur during 1–2 days after the SSC, especially for the IPP (29.8°S, 118.1°E) whose negative anomalous peak value is even up to about 20 TECU on March 17. The anomaly amplitude is much difference at different latitudes. Not only the absolute TEC values are disturbed corresponding to the SSC, but also the hourly standard deviation of the rate of TEC is varied in the next hours of SSC.

As BDS is under construction without many continuous operating tracking stations up to now, BDS GEO TEC monitoring is just at beginning stage. However it has its own advantage for Earth's ionosphere sounding due to its quasi-persistent observation geometry. With the increase of the number of BDS tracking stations, more and more one point TEC series can be obtained with a high time resolution. BDS-GEO TEC monitoring will be greatly contribute to the Earth's ionosphere research, and even become a sensitive detector of ionospheric disturbance in Asia/Pacific region.

# References

1. Hoffmann-Wellenhof B, Lichtenegger H, Collins J (1994) GPS: theory and practice, 3rd edn. Springer, New York
2. Jin SG, Luo O, Park P (2008) GPS observations of the ionospheric F2-layer behavior during the 20th November 2003 geomagnetic storm over South Korea. J Geodesy 82(12):883–892. doi:10.1007/s00190-008-0217-x
3. Jin SG, Wang J, Zhang H, Zhu WY (2004) Real-time monitoring and prediction of the total ionospheric electron content by means of GPS observations. Chin Astron Astrophys 28(3):331–337. doi:10.1016/j.chinastron.2004.07.008
4. Mannucci AJ, Wilson BD, Yuan DN, Ho CH, Lindqwister UJ, Runge TF (1998) A global mapping technique for GPS-derived ionospheric total electron content measurements. Radio Sci 33(3):565–582
5. Schaer S (1999) Mapping and predicting the Earth's ionosphere using the global positioning system. Geod-Geophys Arb Schweiz 59:59
6. Otsuka Y (2001) A new technique for mapping of total electron content using GPS network in Japan. Doctoral dissertation, Kyoto University
7. Hernández-Pajares M, Juan JM, Sanz J, Orus R, Garcia-Rigo A, Feltens J, Krankowski A (2009) The IGS VTEC maps: a reliable source of ionospheric information since 1998. J Geodesy 83(3–4):263–275
8. Bilitza D, McKinnell LA, Reinisch B, Fuller-Rowell T (2011) The international reference ionosphere today and in the future. J Geodesy 85(12):909–920
9. Liu JY, Lin CH, Chen YI, Lin YC, Fang TW, Chen CH, Hwang JJ (2006) Solar flare signatures of the ionospheric GPS total electron content. J Geophys Res: Space Phys 111(A5) (1978–2012)
10. Kumar S, Singh AK (2011) GPS derived ionospheric TEC response to geomagnetic storm on 24 August 2005 at Indian low latitude stations. Adv Space Res 47(4):710–717
11. Occhipinti G, Rolland L, Lognonné P, Watada S (2013) From Sumatra 2004 to Tohoku-Oki 2011: the systematic GPS detection of the ionospheric signature induced by tsunamigenic earthquakes. J Geophys Res Space Phys 118(6):3626–3636
12. Liu JY, Tsai YB, Ma KF, Chen YI, Tsai HF, Lin CH, Lee CP (2006) Ionospheric GPS total electron content (TEC) disturbances triggered by the 26 December 2004 Indian Ocean tsunami. J Geophys Res Space Phys 111(A5) (1978–2012)
13. Ozeki M, Heki K (2010) Ionospheric holes made by ballistic missiles from North Korea detected with a Japanese dense GPS array. J Geophys Res Space Phys 115(A9) (1978–2012)
14. Li ZH, Huang JS (2005) GPS surveying and data processing. Wuhan University Press, China, Wuhan (in Chinese)
15. Datta-Barua S, Walter T, Blanch J, Enge P (2008) Bounding higher-order ionosphere errors for the dual-frequency GPS user. Radio Sci 43(5)